Transactions of the Materials Research Society of Japan 29 [2] 607-610 (2004)

Iron nano-clusters in SiO_2 synthesized by ion implantation and the magnetic properties

T. Moriwaki[1], N. Hayashi[1*], I. Sakamoto[2], H. Tanoue[2], T. Toriyama[3], and H. Wakabayashi[3]
[1]Kurume Institute of Technology, 2228 Kamitsu, Kurume-shi, Fukuoka 830-0052, Japan
[2] National Institute of Advanced Industrial Science and Technology, 1-1-1 Umezono, Tsukuba-shi, Ibaraki 305-8568, Japan
[3] Musashi Institute of Technology, 1-28-1, Tamazutsumi, Setagayaku, Tokyo 158-8557, Japan
Fax: 81-942-22-1345, e-mall:nhayashi@cc.kurume-it.ac.jp

The formation of iron nano-clusters in amorphous SiO_2 by ion implantations was studied. The implantation of ^{57}Fe ions was performed at room temperature up to total dose of 3.0×10^{17} ions/cm^2 with projectiles' energy of 74 keV and 100 keV. It is shown by the measurements of conversion electron Mössbauer spectroscopy and magnetization that the clusters exhibit transitions from superparamagnetic to ferromagnetic states at the dose range of $(1.0 \sim 1.5) \times 10^{17}$ ions/cm^2, whose result indicates that under the same condition of implantation the clusters precipitates rapidly and effectively in SiO_2 at the smaller dose than in α-Al_2O_3 matrices. Furthermore, it is suggested that Si atoms are dissolved into the precipitated iron clusters in the Fe/SiO_2 nano-composites.
(key words; iron clustering, SiO_2 matrix, Fe-Si alloy, Ion implantation)

1. INTRODUCTION

It is well known that nano-crystalline particles exhibit peculiar physical and chemical properties, and, recently, composite system of metal nano-clusters embedded in insulating oxide matrices have attracted much attention because of their unusual optical, electrical, and magnetic properties [1, 2]. The implantation of magnetic metal ions into refractory metal oxides has been used to form such granular films, offering potential important applications in the fields of magnetic recording media, magnetic refrigation, medical diagnostics, and so on. We have presented that the magnetic-buried-granular layers produced by implantation of Fe ions into α-Al_2O_3 and MgO single crystals exhibit an eminent giant magnetoresistance (GMR) [3, 4]. On the one hand, SiO_2 is an attractive substrate material for dispersing metal nano-clusters from the viewpoints of modern electronics, and it should be stressed that ion implantation is a technology capable of synthesizing nano-clusters with controlled size and composition and compatible with silicon device technology. Although a few studies have been reported on the characteristics of SiO_2 implanted with Fe ions at the doses over 1.0×10^{17} ions/cm^2 [5, 6], the physical properties of the iron clusters are still remained unclear. Therefore, it is useful to investigate the magnetic properties in the Fe-SiO_2 composite system (Fe/SiO_2).

In the study reported here we have used conversion electron Mössbauer spectroscopy (CEMS), together with X-ray diffraction and magnetization measurements, to investigate the formation of iron precipitates and the subsequent change in magnetic properties in the surface layers of ^{57}Fe implanted SiO_2 matrices. It is demonstrated that the iron precipitation in the Fe/SiO_2 exhibits different properties than the iron implantation into Al_2O_3 and MgO in respect of both the rapid growth of the iron clusters and Si inclusion in the clusters.

2. EXPERIMENTAL

The sample was prepared by implantation of $^{57}Fe^+$ ions into the amorphous SiO_2 (a-SiO_2) substrate at a dose of $(1.4 \sim 3.0) \times 10^{17}$ ions/cm^2. The energy of the projectiles was 100 keV and 74 keV with current density of a few μA/cm^2. The two energies were chosen to compare the properties of iron granules with those in Fe/Al_2O_3 [4]. The implantation conditions are summarized in Table 1; e.g., the sample A was implanted with the total dose of 1.4×10^{17} ions/cm^2. The crystalline structure of the implanted layers was characterized by glancing angle x-ray diffraction (GXRD). The GXRD patterns were measured with a glancing angle of $\theta = 2.5°$, using Cu targets. CEMS was measured with a He + 4% CH_4 gas flow proportional counter, using a 740 MBq ^{57}Co source in Rh. Mössbauer spectra were analyzed by least-squares fitting with overlapping Lorentzian curves. The magnetic properties were measured with a vibrating sample magnetometer (VSM) where magnetization in granular layers were achieved by applying perpendicular and in-plane external fields H up to 15 kOe. The implantations and all measurements were performed at room temperature.

Table I; Implantation conditions for the samples numbered as A ~ E. The sample numbers are referred in the text

Sample Number	Matrix	Dose at 100keV : [ions/cm^2]	Dose at 74keV : [ions/cm^2]
A	a-SiO_2	1.0×10^{17}	0.4×10^{17}
B	a-SiO_2	0	1.5×10^{17}
C	a-SiO_2	3.0×10^{17}	0
D	c-SiO_2	0	1.5×10^{17}
E	Al_2O_3	1.5×10^{17}	0

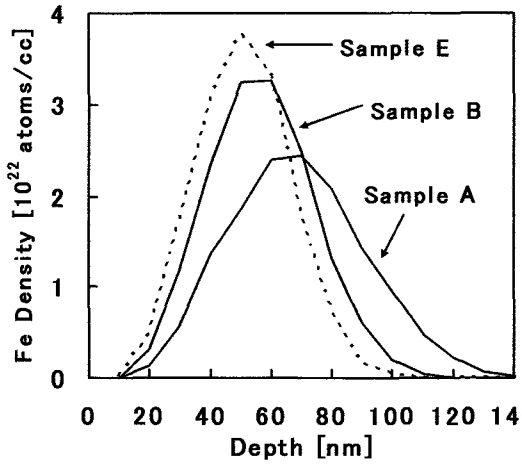

Fig. 1; Fe ions distribution calculated from TRIM code for the sample E (Fe/Al_2O_3), sample B (Fe/SiO_2), and sample A (Fe/SiO_2)

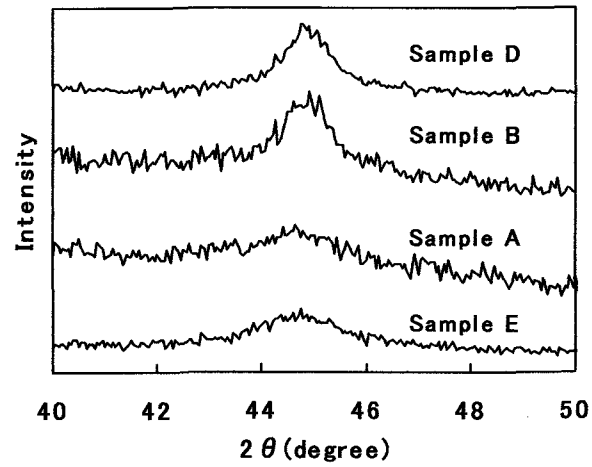

Fig. 2; GXRD patterns from the implanted layers of the, sample A ($Fe/a\text{-}SiO_2$), and sample B ($Fe/a\text{-}SiO_2$), sample D ($Fe/c\text{-}SiO_2$), and sample E (Fe/Al_2O_3).

Fig. 1 shows simulation curves of the Fe distribution calculated by the TRIM code for the samples A, B and E. It is noted in the figure that the ion distribution with 74 keV implantation in SiO_2 substrate is comparable with 100 keV ions in Al_2O_3 and that the implantation with 100 keV and 74 keV (sample A) offers two third peak concentration of the 74 keV implantation (sample B).

3. RESULTS AND DISCUSSION

The structure evolution of the nano-composite films was monitored by XRD, VSM and CEMS, from which some new results are presented.

Fig.2 shows typical GXRD patterns from the implanted layers of SiO_2 substrates, together with that in Al_2O_3 for comparison. A rather sharp peak appears at about $2\theta = 45°$ corresponding to the diffraction from bcc α–Fe (110) planes. The GXRD peaks were analyzed by the least-squares fitting assuming Gaussian curves, and the obtained parameters are summarized in Table II. The lattice parameters of Table II are in agreement with the value of 0.287 nm in bulk α-iron. We have also performed implantation in crystalline SiO_2 ($c\text{-}SiO_2$) substrate in order to investigate whether the crystalline structure of the matrix affects the precipitation of α-iron. The results from Fig.2 and Table II show that there appear to be a little difference between the precipitation in $a\text{-}SiO_2$ and in $c\text{-}SiO_2$, suggesting that the implanted Fe atoms may precipitate through the damaged amorphous matrix. On the other hand, it is noted that at a dose of 1.5×10^{17} ions/cm^2 the size of the nano-particles in the SiO_2 is approximately twice as large as that in Al_2O_3 matrix.

Fig. 3 shows magnetization curves measured for the samples implanted to high doses in SiO_2 matrices. The curves with thick and thin lines denote the magnetization when applying in–plane and perpendicular fields, respectively. We can hardly see the magnetic hysteresis loop and the saturation of magnetization in the sample A, Fig. 3(a). It indicates for the most nano-clusters to be superparamagnetic. But the sample B with a dose of 1.5×10^{17} ions/cm^2 has a clear hysteresis loop for in-plane field, as shown in the inset of Fig. 3(b). For the sample C the hysteresis loops appears eminently for both in–plane and perpendicular fields. The result shows that the nano-clusters grow in the size with increasing dose and exhibit intensive ferromagnetic characteristics. The difference between in-plane and perpendicular magnetization indicates that the average of the easy directions of magnetization are in the implanted plane. It is suggested that the possible source of the magnetic anisotropy is shape anisotropy and that the iron nano-particles are in the shape of oblate ellipsoids [7]. The suggestion is consistent with CEMS measurements whose spectrum shows that the intensities of the second and fifth lines of the magnetic splitting are larger than those of the outer lines as shown in Fig. 4 (b). The values of saturation magnetization in Fig. 3 are much higher than those of Fe/SiO_2 granules reported by Ding' et al. but still lower than that of bulk Fe (~220 emu/g) [5], while the coercivity estimated from Fig. 3(c) is obtained as 127 Oe and is much higher than that of bulk Fe (~10 Oe), maybe due to the uniaxial anisotropy.

Mössbauer spectroscopy is useful to elucidate the physical states of the implanted irons through the

Table II; GXRD parameters obtained for the samples in Fig. 2.

Granules : Dose[ions/cm^2]	2θ	Peak width	Lattice parameter [nm]	Granule's diameter [nm]
1.4×10^{17} (sample A)	44.8°	1.01°	0.286	6
1.5×10^{17} (sample B)	44.9°	0.44°	0.284	15
1.5×10^{17} (sample D)	44.9°	0.51°	0.284	13
1.5×10^{17} (sample E)	44.7°	0.88°	0.286	7

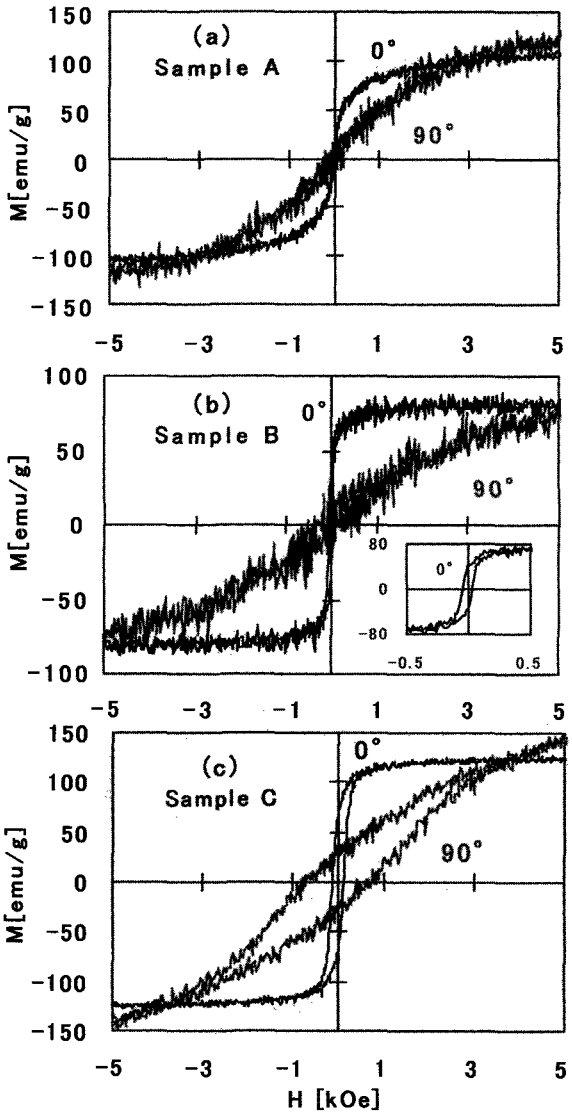

Fig. 3; Magnetization curves taken from iron implanted Fe/a-SiO_2. (a) sample A, (b) sample B, and (c) sample C

measurement of hyperfine parameters. Fig. 4 (a) shows a CEM spectrum taken from the sample A with a total dose of 1.4×10^{17} ions/cm^2 where the clusters' size has been estimated as 6 nm in Table II. The central part of the spectrum was fitted with the assumption of overlapping Lorenzians which consist of one single line and three quadrupole doublets from ferric and two forms of ferrous irons. The doublets assigned to ionic forms of Fe^{3+} and Fe^{2+} are supposed to arise from the iron oxides in complex form [8]. The single line peaked near zero velocity can be ascribed to metallic α-iron aggregates (Fe^0) that exhibit superparamagnetic characteristics due to its small size in nanometer scale [9]. A set of magnetic sextet lines was added to fit the fringe on the central peaks in Fig. 4. The appearance of the sextet suggests that among the superparamagnetic granules the ferromagnetic nano-particles are evolved in the dispersion of Fe/SiO_2 composites even at such a low dose as 1.4×10^{17} ions/cm^2.

It is shown in Fig. 4 (b) that the magnetic sextets, i.e., ferromagnetic component of Fe^0, appear clearly at the expense of superparamagnetic Fe^0 components for the

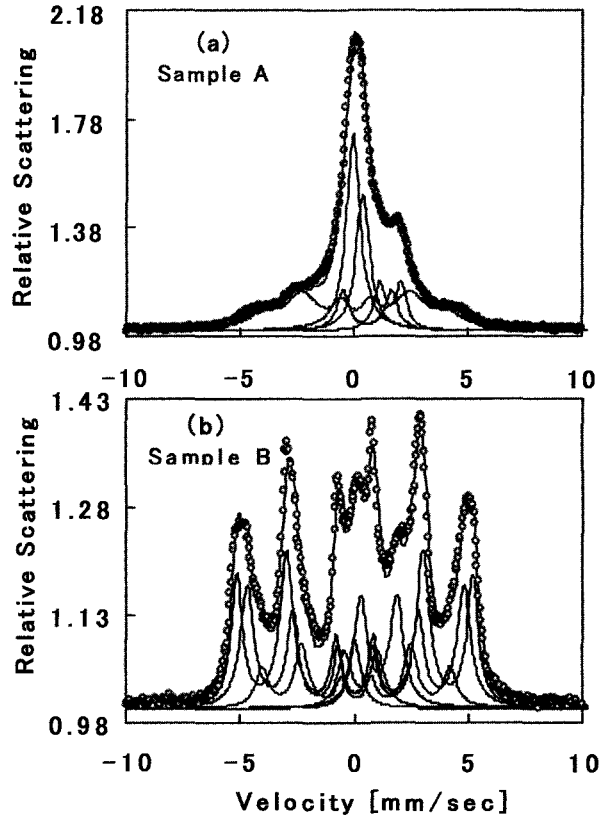

Fig. 4 ; CEM spectra of the Fe/a-SiO_2 granules for the sample A, (a), and sample B, (b).

Table III; Mössbauer parameters of iron nano-particles present in implanted Fe/SiO_2 samples, obtained from Fig. 4(b). *IS* is the isomer shift and B_{hf} the internal field. The column* shows the B_{hf} change relative to the site 1.

Sample	Parameters	Site 1	Site 2	Site 3
Implanted Fe/a-SiO_2	B_{hf} [kOe]	321	296	256
	$B_{hf,n}/B_{hf1}$*	1.00	0.920	0.797
	I.S. [mm/s]	0.026	0.057	0.084
Bulk Fe-Si alloys	B_{hf1}/B_{hfFe}*	1.00	0.917	0.834
	I.S. [mm/s]	0.01	0.03	0.09

sample B with an increased dose of 1.5×10^{17} ions/cm^2. The result demonstrates that most of the iron nano-particles precipitate in ferromagnetic state due to the size increase with increasing dose. On the other hand, we have shown that in Fe/Al_2O_3 composites the critical size of Fe^0 granules where the superparamagnetic relaxation is blocked at room temperature is achieved at the dose of $(1.5 \sim 2.0) \times 10^{17}$ ions/cm^2. Thus, the ferromagnetic clusters appear at the smaller dose by 0.5×10^{17} ions/cm^2 than in Fe/Al_2O_3, indicating that the implanted irons aggregate rapidly and effectively in the SiO_2 matrices. The result is in good agreement with the results of XRD and VSM measurements. Judging from Table II, the critical size for the blocking of superparamagnetic relaxation seems to be around or more than 6 nm.

Fe-Si alloys have been the materials of great interest

for many decades and alloys of the low silicon region have been well investigated for practical uses. It is well known that the disordered alloys with 0 ~ 10 at. % Si show separate internal magnetic fields, B_{hf}, from Fe atoms with different nearest neighbours of solute Si and that the chemical isomer shift in the alloys increases regularly with increase in Si of nearest neighbours . The spectrum in Fig. 4 exhibits ferromagnetic splitting with three resolvable internal magnetic fields whose pattern is very similar to that observed for disordered Fe-Si bulk alloys [10]. The hyperfine parameters obtained from the analysis for the ferromagnetic iron clusters are summarized in Table III. The B_{hf} value of 321 kOe for the site 1 is close to that of bulk iron, 330 kOe, and the difference of 10 kOe is caused by collective excitation of the nano-particles [9]. It is clearly demonstrated that the relative change in both internal fields and isomer shifts for the sites 2 and 3 are in good agreement with those measured in bulk alloys. Therefore, the three sites are considered to correspond to the Fe atoms which have 8, 7 and 6 nearest-neighbor Fe; i.e., the latter two cases correspond to one and two Si atoms substitution for the iron sites in the bcc lattice. The Si concentration is estimated to be in the range of 5 ~ 10 at. %, judging from the intensity of the site 3 [10]. The Si atoms are supposed to be taken part in the iron precipitation from SiO_2 matrix during collision cascades of ion implantation. The alloy formation is consistent with the result of XRD measurements, i.e., the decrease in lattice parameters of the Fe/SiO_2 composite, because the lattice constant decreases by only 0.3 % with alloying of 10 at. % Si. It is noteworthy that in the case of Fe/Al_2O_3 granules the iron clusters never include Al from the matrix element during ion implantation because the ferromagnetic clusters are characterized by only one internal magnetic field [11].

We would expect a significant GMR effect in the Fe/SiO_2 granular layers prepared by ion implantation to the dose of 1.4×10^{17} ions/cm^2 since an amount of superparamagnetic nano-particles exists there, and actually the magnetization measured by VSM was comparable to that observed in the Fe-implanted Al_2O_3 granules [3]. MR ratios in the iron granules prepared by implantation were observed to be 7.5 % for Fe/Al_2O_3 and 3.5 % for Fe/MgO for H = 12 kOe [3, 4]. Furthermore, the MR ratio in the granular Fe/SiO_2 films prepared by rf sputtering was observed to be (2 ~ 3) %, depending on Fe content [12]. However, the MR ratio in the implanted Fe/SiO_2 was observed to be 1 % at most for H = 10 kOe. The difference of GMR evolution could be attributed to the dispersion states of Fe nano-clusters in the implanted layer. It is likely that the bigger size of the nano-clusters causes the larger separation between the clusters in Fe/SiO_2 than in Fe/Al_2O_3 and sputtered Fe/SiO_2 film, and leads to the decrease of electron tunneling probability and then the GMR effects. We can say that the rapid growth of the iron precipitation in the implanted Fe/SiO_2 layers causes the lowering of the GMR effect. The characteristic growth process of the nano-clusters in the implanted Fe/SiO_2 will be discussed in the future report.

4. CONCLUSION

Ion implantation was used to modify magnetic properties in the surface layers of amorphous SiO_2 and investigated by combined methods of X-ray diffraction, magnetization measurement and Mössbauer spectroscopy. The prepared granules exhibit from superparamagnetic to ferromagnetic transition at a smaller dose than that in Fe/Al_2O_3, which means rapid growth of the nano-clusters in the implanted SiO_2 matrix. Most of the nano-particles are in ferromagnetic state at the dose of 1.5×10^{17} ions/cm^2. We have found that an amount of Si atoms are mixed in the iron precipitation during ion implantation to form Fe-Si alloys in the nano-clusters.

ACKNOWLEDGMENTS

A part of this study was financially supported by the Yoshida Foundation for the Promotion of Learning and Education (Kurume).

REFERENCES

[1] C.E. Vallet, C.W. White, S.P. Withrow, J.D. Budal, L.A Boatner, K.D. Sorge, J.R. Thmpson, K.S. Beaty and A. Meldrum, J. Appl. Phys. , **92,** 6200- 04 (2002).
[2] G.L. Zhang and H. Pattyn, Hyperfine Interact., **113** , 165- 181 (1998)
[3]. N. Hayashi, I. Sakamoto, H.Tanoue, H.Wakabayashi, and T. Toriyama, Hyperfine Inter., **158/159**, 193- 97 (2003).
[4] N. Hayashi, I. Sakamoto, T. Toriyama, H. Wakabayashi, T. Okada, and K. Kuriyama, Surface and Coating Techno., **169/170,** 540-43 (2003).
[5] Xing-zhao Ding, B.K. Tay, X.Shi, M.F. Chiah, W.Y. Cheung, S.P. Wong, J.B. Xu, and I.H. Wilson, J. Appl. Phys., **88**, 2745-49 (2000).
[6] A. Perez, M. Treilleux, T. Capra, and D.J. Criscom, J. Mater. Res., 2, 910-917 (1987).
[7] H. Wakabayashi, T. Hirai, T. Toriyama, N. Hayashi, and I. Sakamoto, Phys. Status Solidi A, 94, 515-520 (2002).
[8] C.J. McHargue, P.S. Sklad, C.W. White, G.C. Farlow, A. Perez, and G. Marest, J. Mater. Res., **6**, 2145- 2159 (1991)
[9] F. Bodker and S. Morup, Hyperfine Interact., **93**, 1421- 25 (1994)
[10] M.B. Stearns, Phys. Rev.. **129,** 1136-1144 (1963)
[11] N. Hayashi, I. Sakamoto, H. Tanoue, H. Wakabayashi, and T. Toriyama, J. Appl. Phys., **94,** 2597-601 (2003).
[12] S. Honda, T. O. Okada, M. Nawate, and M. Tokumoto, Phys. Rev., **56,** 14556- 563 (1997).

(Received October 9, 2003; Accepted January 20, 2004)